

Review

## Non-Stoichiometric Polymer-Cyclodextrin Inclusion Compounds: Constraints Placed on Un-Included Chain Portions Tethered at Both Ends and Their Relation to Polymer Brushes

Alan E. Tonelli

Fiber & Polymer Science Program, College of Textiles, North Carolina State University, Campus Box 8301, Raleigh, NC 27695-8301, USA; E-Mail: atonelli@ncsu.edu; Tel.: +1-919-515-6588; Fax: +1-919-515-6532

Received: 16 May 2014; in revised form: 25 June 2014 / Accepted: 15 July 2014 /

Published: 13 August 2014

---

**Abstract:** When non-covalently bonded crystalline inclusion compounds (ICs) are formed by threading the host cyclic starches, cyclodextrins (CDs), onto guest polymer chains, and excess polymer is employed, non-stoichiometric (n-s)-polymer-CD-ICs, with partially uncovered and “dangling” chains result. The crystalline host CD lattice is stable to ~300 °C, and the uncovered, yet constrained, portions of the guest chains emanating from the CD-IC crystal surfaces behave very distinctly from their neat bulk samples. In CD-IC crystals formed with  $\alpha$ - and  $\gamma$ -CD hosts, each containing, respectively, six and eight 1,4- $\alpha$ -linked glucose units, the channels constraining the threaded portions of the guest polymer chains are ~0.5 and 1.0 nm in diameter and are separated by ~1.4 and 1.7 nm. This results in dense brushes with ~0.6 and 0.4 chains/nm<sup>2</sup> (or 0.8 if two guest chains are included in each  $\gamma$ -CD channel) of the un-included portions of guest polymers emanating from the host CD-IC crystal surfaces. In addition, at least some of the guest chains leaving from a crystalline CD-IC surface re-enter another CD-IC crystal creating a network structure that leads to shape-memory behavior for (n-s)-polymer-CD-ICs. To some extent, (n-s)-polymer-CD-ICs can be considered as dense polymer brushes with chains that are tethered on both ends. Not surprisingly, the behavior of the un-included portions of the guest polymer chains in (n-s)-polymer-CD-ICs are quite different from those of their neat bulk samples, with higher glass-transition and melt crystallization temperatures and crystallinities. Here we additionally compare their behaviors to samples coalesced from their stoichiometric ICs, and more importantly to dense polymer brushes formed by polymer chains chemically bonded to surfaces at only one end. Judging on the basis of their glass-transition, crystallization and melting temperatures, and crystallinities, we generally find the un-included portions of

chains in (n-s)-polymer-CD-ICs to be more constrained than those in neat bulk as-received and coalesced samples and in high density brushes. The last observation is likely because many of the un-included chain portions in (n-s)-polymer-CD-ICs are tethered/constrained at both ends, while the chains in their dense brushes are tethered at only one end.

**Keywords:** tethered polymers; cyclodextrins; inclusion compounds; brushes

## 1. Introduction

Cyclodextrins (CDs) are cyclic starches containing 6( $\alpha$ ), 7( $\beta$ ), or 8( $\gamma$ ) 1,4- $\alpha$ -linked glucose units (see Figure 1) and are well known for their abilities to form non-covalently bonded inclusion compounds (ICs) with a variety of guest molecules, including polymers [1]. Polymer-CD-ICs are formed by the host CDs threading over guest polymer chains and forming crystals with columns of CDs packed closely together (see Figure 2). Each crystalline column contains guest polymer chains in the channels created by the cavities of the CDs resting on each other.

More than a decade ago Inoue and co-workers [2] first reported the formation of a non-stoichiometric-polymer-cyclodextrin-inclusion compound [(n-s)-Polymer-CD-IC] (see bottom of Figure 2) between excess guest poly (3-hydroxybutyrate) (PHB) and host  $\alpha$ -CD. They observed the un-included portions of the PHB chains to crystallize more rapidly from the melt at significantly higher temperatures than neat bulk PHB. For this reason small quantities of the (n-s)-PHB- $\alpha$ -CD-ICs were used to nucleate the melt-crystallization of neat bulk PHB, and they showed that the resulting semi-crystalline morphology was improved with smaller and more homogeneously dispersed crystalline regions. Shortly thereafter, Vogel *et al.* [3] demonstrated that melt-spun PHB fibers nucleated with (n-s)-PHB- $\alpha$ -CD-IC in this manner evidenced greatly enhanced tensile strengths.

**Figure 1.** Cyclodextrin (CD) and Urea (U) hosts used for forming polymer-inclusion compounds (ICs).

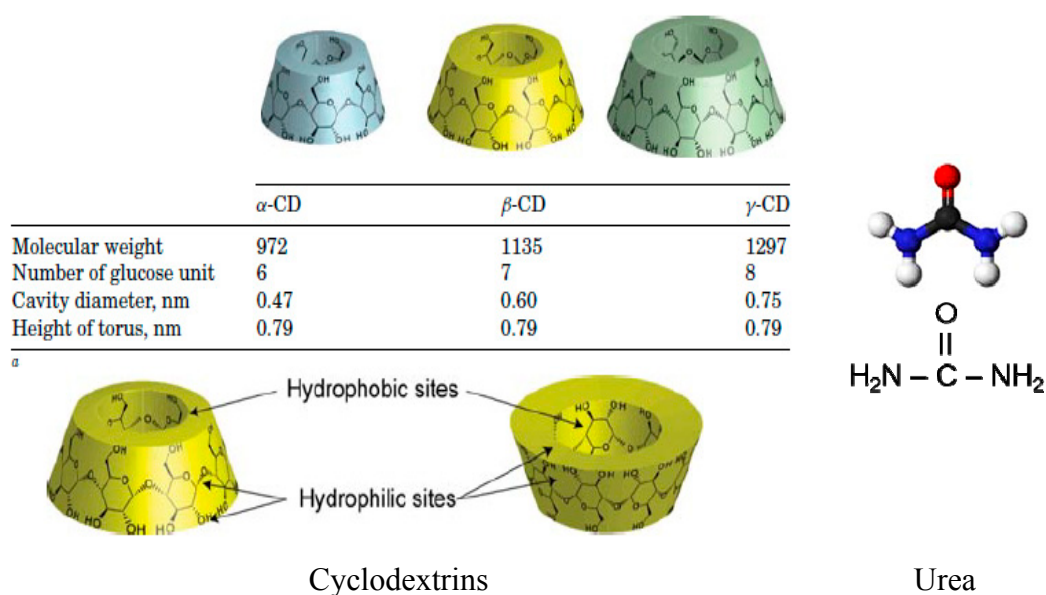
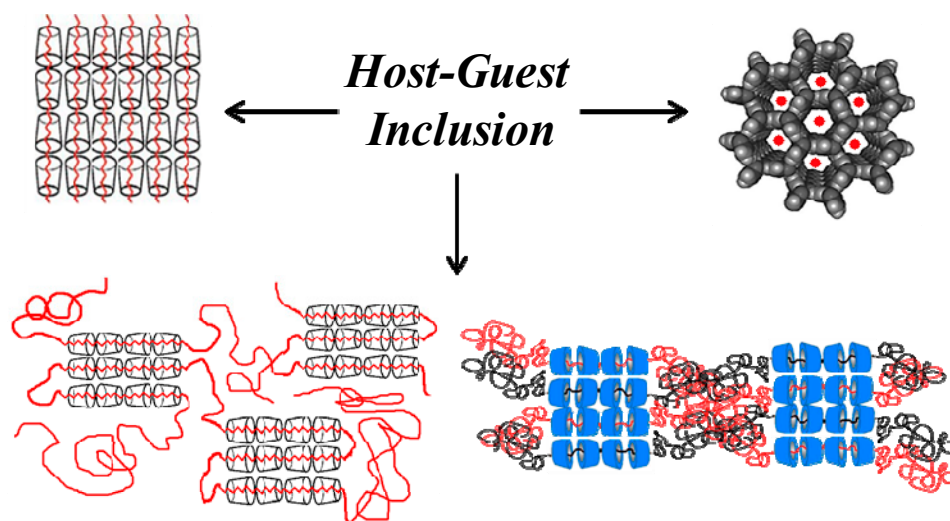


**Figure 2.** Polymer CD-ICs. (top left) and (top right) stoichiometric CD- and urea-ICs; (bottom left) and (bottom right) (n-s)-neat and common mixed CD-ICs.



Since that time Inoue and co-workers have investigated the formation and behaviors of several other (n-s)-polymer-CD-ICs [4–7], including the dependence of their behaviors on host:guest stoichiometries, the molecular weights of the guest polymers, and their “shape-memory” behavior.

Our research group began to examine the formation, behaviors, and uses of (n-s)-polymer-CD-ICs [8–13] by forming them with both  $\alpha$ - and  $\gamma$ -CD hosts and guest nylon-6 with different molecular weights obtained by anionic ring-opening polymerization of  $\epsilon$ -caprolactam [8,9]. Similar to Inoue *et al.* we found (n-s)-nylon-6-CD-ICs to effectively nucleate the melt crystallization of neat bulk nylon-6, leading to improved mechanical properties [9,10]. We subsequently used such nucleated nylon-6 as the reinforcement for as-received nylon-6 matrices to form single polymer composites with necessarily compatible and strong interfaces [10]. In addition, the “shape-memory” of our (n-s)-nylon-6-CD-ICs was demonstrated by heating them above the melting temperatures ( $T_m$ s) of the un-included nylon-6 chain portions, deforming and quenching the deformed sample, and finally reheating above  $T_m$  and regaining the original un-deformed sample shape [9].

Similar film sandwich composites were also made using poly( $\epsilon$ -caprolactone) (PCL) [11], but in this case the reinforcement was PCL self-nucleated with small amounts of PCL that were coalesced from their stoichiometric fully covered  $\alpha$ -CD and urea (U)-ICs. This was prompted by observations [12] that, like the un-included chain portions in (n-s)-polymer-CD-ICs, crystallizable polymers coalesced from their stoichiometric ICs by careful removal of host CDs or urea (U) crystallize more rapidly and at higher temperatures from their melts than un-nucleated neat samples.

Here we focus on the comparison of the behaviors of the un-included guest polymer chain portions in neat (n-s)-polymer-CD-ICs to those exhibited in their common (n-s)-CD-ICs (see Figure 2 bottom) containing two different guest polymers, their neat bulk samples, as-received and coalesced from their stoichiometric ICs, and most importantly to the behaviors of polymer chains in their dense brushes. As indicated in Figure 2 (Top), and which will be more thoroughly discussed below, the density of chains leaving the surfaces of (n-s)-Polymer-CD-IC crystals are comparable to those of high density polymer brushes. Our purpose is to compare the degrees of constraint experienced by the polymer chains in these different sample forms, with special emphasis placed on the differences produced by

tethering chains at a single end and both chain ends, as occurs, respectively, in polymer brushes and in (n-s)-polymer-CD-ICs.

## 2. Experimental Section

The methods used to form and characterize stoichiometric polymer-ICs made with CD and urea (U) hosts (see Figure 2) and (n-s)-polymer-CD-ICs have been described many times [8–13] and will not be repeated here. Instead we briefly describe the techniques and instruments used to probe the un-included portions of the guest chains in (n-s)-CD-ICs and polymer samples coalesced from their stoichiometric CD- and U-ICs.

### *Materials and Methods*

Atactic poly(methyl methacrylate) (PMMA) ( $M_w = 350$  kDa), atactic poly(vinyl acetate) (PVAc) ( $M_w = 167$  kDa), and urea (U) were purchased from Sigma-Aldrich Co. (St. Louis, MO, USA),  $\gamma$ -CD was obtained from Wacker Silicones (Adrian, MI, USA), and dioxane was obtained from Fischer Scientific (Hampton, UK). Differential Scanning Calorimetry (DSC) was employed to characterize the (n-s)-ICs and coalesced polymers. A PerkinElmer Diamond DSC-7 (PerkinElmer, Inc., Waltham, MA, USA) and TA Instruments Q1000 DSC (New Castle, DE, USA) were used to perform thermal scans. DSC scans followed a Heat-Cool-Heat profile, with samples held above their glass transition and melting temperatures after the first heating scan for a substantial amount of time to remove prior processing history. Heating and cooling rates of 20 °C/min were typically used. As-received- (asr-) and coalesced- (c) polymers and their (n-s)-CD-IC samples were heated at 5 °C/min and then rapidly cooled at 50 °C/min, and nitrogen was used as the purge gas. All DSC data were analyzed with PerkinElmer's Pyris software.

Densities were measured on films by a flotation method using water and its mixtures with 40 wt% NaBr, which have densities of 0.9982 and 1.4138 g/cm<sup>3</sup>, respectively, at 25 °C [14].

## 3. Results and Discussion

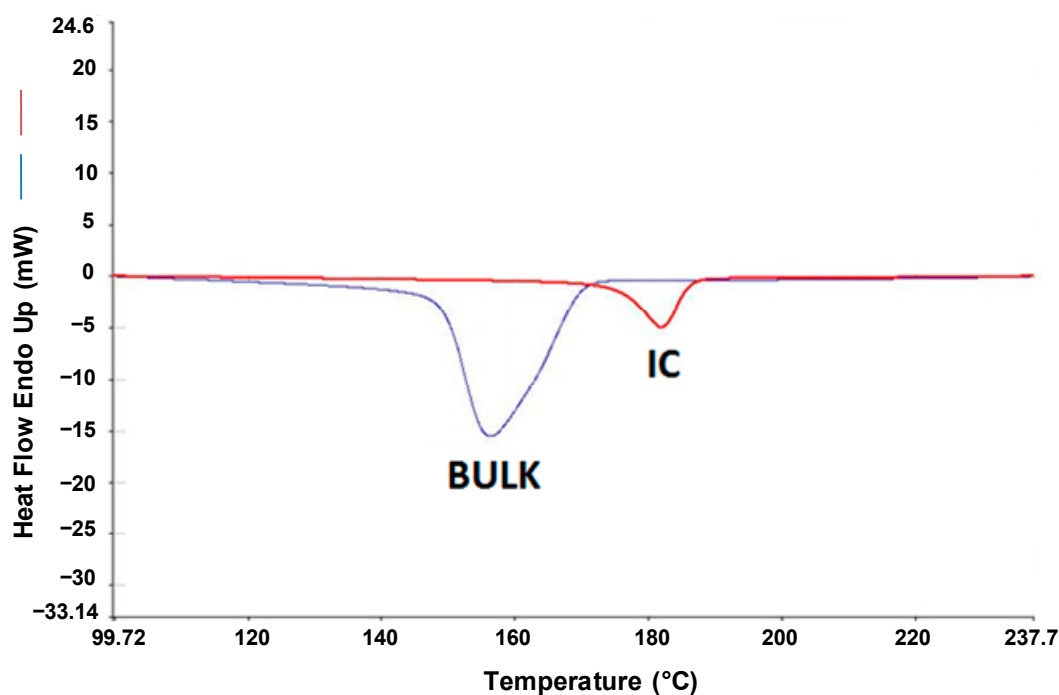
### *3.1. Semi-Crystalline Polymers in (n-s)-CD-ICs and Coalesced from Their Stoichiometric ICs*

We begin by summarizing the formation and behaviors of (n-s)-ICs containing guest nylon-6 samples of various molecular weights and  $\alpha$ - and  $\gamma$ -CD hosts [8,9]. Nylon-6 (N-6) samples with  $M_w = 30,000$  and 60,000 Da were obtained from BASF (Ludwigshafen, Germany), while those with  $M_w = 300,000$  and 600,000 Da were obtained by anionically initiated ring-opening polymerization of  $\epsilon$ -caprolactam [15]. It should be noted that single and two side-by-side nylon-6 chains [16] are, respectively, threaded through  $\alpha$ - and  $\gamma$ -CDs.

The melt crystallization behavior shown in Figure 3 for the 3:1 (n-s)-N-6- $\gamma$ -CD-IC cooled at 10 °C/min in the DSC is typical for all the (n-s)-N-6-CD-ICs examined. Note that, upon cooling from the melt, the un-included chain portions in the (n-s)-IC sample crystallize before,  $T_c \sim 30$  °C higher, than the neat bulk sample. It was also observed that a higher fraction or proportion of the un-included N-6 chain portions “dangling” from the 3:1 (n-s)- $\alpha$ -CD-IC crystals are able to crystallize compared to the neat N-6 melt. Qualitatively similar observations were made for 6:1 N-6- $\gamma$ -CD-IC and

bulk samples, with N-6 of  $M_w = 600,000$ . As the N-6  $M_w$  increased, the constraints on the “dangling” chains in 3:1 (n-s)-N-6- $\alpha$ -CD-ICs increasingly facilitate their crystallization in comparison to their neat melts, which, to the contrary, generally crystallize less readily as their  $M_w$ s increase. Also note that the “dangling” chain portions in the (n-s)-nylon-6- $\gamma$ -CD-ICs showed elevated  $T_c$ s as well.

**Figure 3.** Differential Scanning Calorimetry (DSC) cooling scans from the melts of 600,000 Da bulk N-6 and its 3:1 (n-s)- $\gamma$ -CD-IC [8].



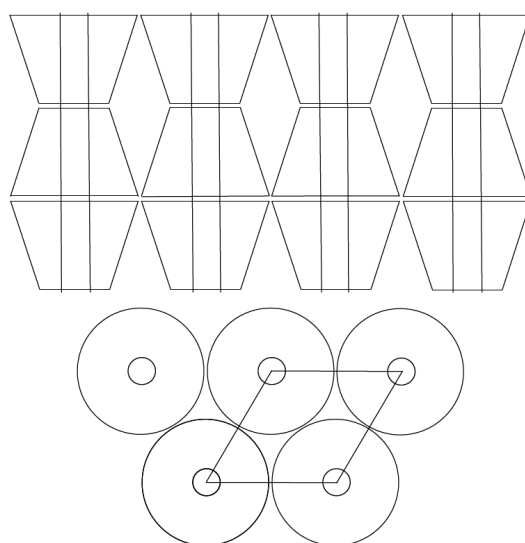
Observations that the un-included, uncovered N-6 chain portions in both 3:1  $\alpha$ -CD- and 6:1  $\gamma$ -CD-ICs show  $X_c$ s and  $T_c$ s that are increased in comparison to the 2:1 N-6- $\alpha$ -CD- and 4:1 N-6- $\gamma$ -CD-ICs are in agreement with the results reported for (n-s)-poly(butylene succinate) (PBS)- $\alpha$ -CD-ICs [6,17]. Actually N-6 chains dangling from (n-s)-N-6- $\alpha$ - and  $\gamma$ -CD-ICs with stoichiometries less than 3:1 and 6:1, respectively, were observed to crystallize less readily than their neat bulk samples.

A more germane measure of the crystallizability of bulk and un-included “dangling” N-6 chains was suggested to be provided by comparing “dangling” N-6 chains of the same length ( $M_w$ ) as the bulk N-6. As an example, the N-6 chains “dangling” from the 4:1 N-6 (600,000)- $\gamma$ -CD-IC crystals should on average have a length characterized by  $M_w = 300,000$ , because the 2:1 N-6- $\gamma$ -CD-IC is stoichiometric, with no un-included “dangling” chain portions. The 2:1 N-6 (600,000)- $\alpha$ -CD-IC should also have “dangling” chains of average  $M_w = 300,000$ . Bulk N-6 (300,000); 2:1 N-6 (600,000)- $\alpha$ -CD-IC; and 4:1 N-6 (600,000)- $\gamma$ -CD-IC showed, respectively,  $X_c$ ,  $T_c = 0.23$ , 174; 0.15, 173; and 0.16, 162 °C,. Thus, N-6 chains “dangling” from both (n-s)-CD-ICs did not show enhanced crystallizability compared with bulk N-6 with  $M_w = 300,000$ . Except for those between the chains “dangling” from 3:1 and 6:1 N-6- $\alpha$ - and  $\gamma$ -CD-ICs and bulk N-6 with the same  $M_w$ s, this observation held for other like comparisons. In opposition to observations reported [17] for (n-s)-PBS- and poly-( $\epsilon$ -caprolactone) (PCL)- $\alpha$ -CD-ICs, however, as the N-6:CD ratio increased, the crystallinity  $X_c$  (of the un-included chain portion) increased.

Even though  $\Delta H_c [(n-s)\text{-CD-IC}]/\Delta H_c (\text{bulk}) = X_c [(n-s)\text{-CD-IC}]/X_c (\text{bulk})$  increased with N-6  $M_w$  for 3:1  $\alpha$ - and 6:1  $\gamma$ -CD-ICs, their values of  $(T_c ((n-s)\text{-CD-IC}) - T_c (\text{bulk}))_s$  did not. In other words, as the  $M_w$  of N-6 increased, the levels of crystallinity achieved for the un-included yet constrained “dangling” chains in their (n-s)-CD-ICs increased in comparison to their neat melts. At the same time, even though they generally crystallized at temperatures higher than bulk samples, their rates of crystallization did not increase [9].

Consider the constraints placed on un-included N-6 chains “dangling” from their (n-s)- $\alpha$ -CD-ICs, as they emerge from  $\sim 0.5$  nm channels separated by  $\sim 1.4$  nm, as indicated below in Figure 4, to those experienced by the pair of closely adjacent N-6 chains in each  $\sim 1$  nm  $\gamma$ -CD-IC channel, separated by  $\sim 1.7$  nm. The distinct behaviors observed for (n-s)-N-6-CD-ICs made with  $\alpha$ - and  $\gamma$ -CDs—lower  $T_c$ s and  $\Delta H_c$ s for (n-s)-N-6- $\gamma$ -CD-ICs—can in part be attributed to the differences in the constraints imposed on their un-included chains “dangling” from their CD-IC channels. Because, in fact, they form dense brushes [18] that do not significantly “dangle”, but are largely extended and parallel, and will be discussed further below.

**Figure 4.** Channel structure of a columnar CD-IC, with 0.6 ( $\alpha$ -CD), 0.8 ( $\gamma$ -CD) N-6 chains/nm<sup>2</sup> of CD-IC crystal surface. Threaded chains are  $\sim 1.5$ – $1.8$  nm apart, so the protruding N-6 chains form dense polymer brushes [18] (For comparison, in the  $\alpha$ -form bulk crystal there are 1.4 N-6 chains/nm<sup>2</sup>) [8].



Single and pairs of side-by-side N-6 chains included, respectively, in the nylon- $\alpha$ - and  $\gamma$ -CD-IC channels emerge from them immediately above their crystalline CD-IC surfaces, with initial channel densities of  $\sim 4$  and  $\sim 3$  nylon-6 chains/nm<sup>2</sup> of channel, respectively. Relative to the entire crystalline surface, or farther above the surface, the density of N-6 chains protruding above them is only modestly greater for the (n-s)- $\gamma$ -CD-ICs (0.8 ( $\gamma$ ) vs. the 0.6 ( $\alpha$ ) nylon-6 chains/nm<sup>2</sup> of IC crystal surface).

We observed the N-6 chains protruding from their 6:1 (n-s)- $\gamma$ -CD-ICs to be only minimally more crystallizable (higher  $T_c$ s, but comparable  $\Delta H_c$ s) than bulk N-6, while significantly less crystallizable than the N-6 chains protruding from their 3:1 (n-s)- $\alpha$ -CD-ICs. Apparently the pairs of side-by-side N-6 chains emerging from each (n-s)- $\gamma$ -CD-IC channel are less able to crystallize than the single chains emerging from each (n-s)- $\alpha$ -CD-IC channel.

The density of an emerging pair of N-6 chains just above the surface of the (n-s)- $\gamma$ -CD-IC crystals is much greater ( $\sim 3/\text{nm}^2$  of  $\gamma$ -CD channel vs.  $1.4/\text{nm}^2$  in the bulk crystal) than the N-6 chain density farther above the (n-s)- $\gamma$ -CD-IC crystal surfaces ( $0.6$  ( $\alpha$ )- $0.8$  ( $\gamma$ ) chains/ $\text{nm}^2$ ), or for that matter in dense polymer brushes. This could result in strong associations, such as hydrogen bonding, between pairs of emerging side-by-side N-6 chains. This may retard their interactions/crystallization with other such closely and strongly interacting pairs of N-6 chains emerging from nearby  $\gamma$ -CD-IC channels.

This suggestion can also be made based on the comparison of two chain “one-dimensional N-6 nano-crystals” with multi-chain “three-dimensional N-6 micro-crystals”, with the former resulting from pairs of side-by-side chains included and initially emerging from the  $\gamma$ -CD-IC channels. If viable, then as the lengths ( $M_{\text{ws}}$ ) of the chains protruding from N-6-(n-s)- $\gamma$ -CD-ICs are reduced, the constraint opposing crystallization produced by the pairs of N-6 chains emerging from the  $\gamma$ -CD-IC channels should increase making their crystallization more difficult.

As the lengths of N-6 chains or their  $M_{\text{ws}}$  increase, generally their melt-crystallization temperatures  $T_c$  decrease/increase and the levels of crystallinity  $X_c$  decrease/increase, respectively, for bulk and (n-s)-CD-IC samples. For neat molten polymers, the increased entanglement between higher  $M_{\text{w}}$  chains and the structural defects they produce are generally cited [19] as reasons that they may crystallize more slowly and not as completely as samples with lower  $M_{\text{ws}}$ . Since the opposite behavior is observed for the un-included “dangling” yet constrained chains in (n-s)-N-6-CD-ICs, their degree of entanglement, if any, is apparently not important to their ability to crystallize. Their relative center-of-mass diffusion is limited by the constraining CD-IC crystals from which they emerge. Thus, entanglement and un-entanglement of the dangling chains, would be expected to be significantly retarded in comparison to that in unconstrained neat molten N-6 samples. DSC observations of (n-s)-N-6-CD-ICs, such as those presented in Figure 3, but not presented here, remain unchanged upon subsequent repeated heating/cooling scans, which suggests the absence of CD de-threading.

We believe the major factor contributing to the enhanced melt crystallizability observed for the protruding N-6 chains (higher  $T_c$ s and larger  $\Delta H_c$ s and  $X_c$ s), as their  $M_{\text{ws}}$  increase, is likely due to the concomitant increase in their extension and orientation with respect to the CD-IC crystal surfaces. Though seemingly discordant with the well-known behavior of most polymer brushes [18], whose chains lose orientation perpendicular to and extension from their surfaces as their  $M_{\text{w}}$  increases, and which initiates a brush-to-mushroom transition, it must be remembered that polymer brushes are generally formed with non-crystallizable polymers and at lower surface densities than the  $0.6$ – $0.8$  N-6 chains/ $\text{nm}^2$  emanating from the (n-s)-N-6-CD-IC crystal surfaces. Furthermore, and probably more important, many of the un-included chain portions in (n-s)-CD-ICs both begin and terminate in CD-IC crystals, and so their constraints would correspond to dense polymer brushes covalently bonded to parallel separated solid surfaces.

At higher brush densities, similar to those expected for (n-s)-polymer- $\gamma$ -CD-ICs (see Figures 1,2,4), it has been observed [18,20] that even the chains in non-crystallizing brushes are highly extended and, thus, highly aligned, perpendicular to the surfaces of their attachment, and increasingly so as  $M_{\text{w}}$  increases. Particularly for the 3:1  $\alpha$ - and 6:1  $\gamma$ -CD-ICs, this could explain the observed enhancement of their crystallizability, both kinetically and thermodynamically, with increased  $M_{\text{w}}$  of the protruding N-6 chains. Whether the protruding N-6 chains begin crystallizing near the CD-IC crystalline surfaces

or farther removed and nearer to their “free” chain ends [9] each would favor the enhancement of their crystallization as their  $M_w$ s increase.

It is apparent that portions of N-6 chains that are un-included and protrude from their (n-s)-CD-ICs crystallize more readily (faster at higher temperatures, over a narrow temperature range, and to greater extents) than bulk N-6 chains. However, the melting temperatures,  $T_m$ , of their resulting crystals are very similar.  $T_m = \Delta H_m/\Delta S_m$ , is the ratio of the enthalpy to the entropy of melting. Apparently this ratio is very similar for N-6 chains in bulk and those constrained by and protrude from (n-s)-CD-IC crystals. This is surprising because we expect in the melt that N-6 chains protruding from the surfaces of their (n-s)-CD-ICs likely constitute a high density brush with largely extended chains, which are expected to possess less conformational entropy than an unconstrained neat N-6 melt. The  $\Delta S_m$  of polymers is generally dominated by the difference in the intramolecular conformational entropies,  $\Delta S_{conf}$ , of their randomly coiling molten and highly extended and conformationally restricted crystalline chains [21–27]. Thus, we would expect the melting of the crystals formed by the nylon-6 chains protruding from their (n-s)-CD-ICs to have smaller  $\Delta S_{conf} \sim \Delta S_m$ , and therefore, higher  $T_m$ s than neat nylon-6 crystals.

The melting of N-6 chains protruding from their (n-s)-CD-ICs is apparently accompanied by  $\Delta H_m$ s that are similarly reduced, because they show  $T_m$ s close to neat samples. The greater extension and orientation of chains expected in their dense brush-like arrangement in the melt, which likely increases the interactions between molten un-included N-6 chains, in comparison to their neat melts, would serve to lower the difference in enthalpies ( $\Delta H_m$ ) between crystalline and molten N-6 chains protruding from the surfaces of their (n-s)-CD-IC crystals.

Though crystallization and melting data for high density brushes composed of semi-crystalline polymers is sparse [28–31], it appears that their  $T_c$ s and  $T_m$ s are much closer and similar, respectively, to those of their bulk samples than have been observed for the un-included constrained chain portions of the polymer chains in their (n-s)-CD-ICs. This may at least be partly a consequence of the fact that at least some of the un-included polymer chains in (n-s)-CD-IC are constrained at both ends, because they thread into and out of the same or two different CD-IC crystals, causing, in the latter case, “Shape-Memory” behavior.

Similar to (n-s)-polymer-CD-ICs, it has been observed [4,9,12] that guest polymers coalesced from their ICs (see Figures 5 and 6) upon careful removal of the host crystalline lattice also crystallize more rapidly and at higher temperatures from their melts than neat as-received bulk samples of the same polymer. Consequently, they, along with (n-s)-polymer-CD-ICs, may be used as effective self-nucleants [9–13]. Melt nucleation of as-received bulk polymers with small amounts of the same coalesced polymer has an important advantage over (n-s)-polymer-CD-ICs. Self-nucleation with coalesced polymers does not introduce any CDs, and therefore serves as a “stealth” means of nucleation and provides polymer samples that may be used for medical implantation and that are easily recycled, as well.



**Figure 5.** Mechanisms of polymer-IC formation with CD and U hosts [32].

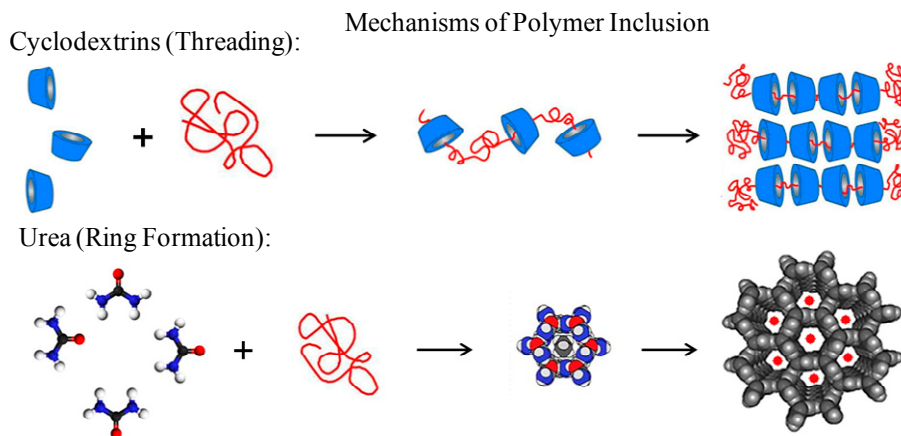
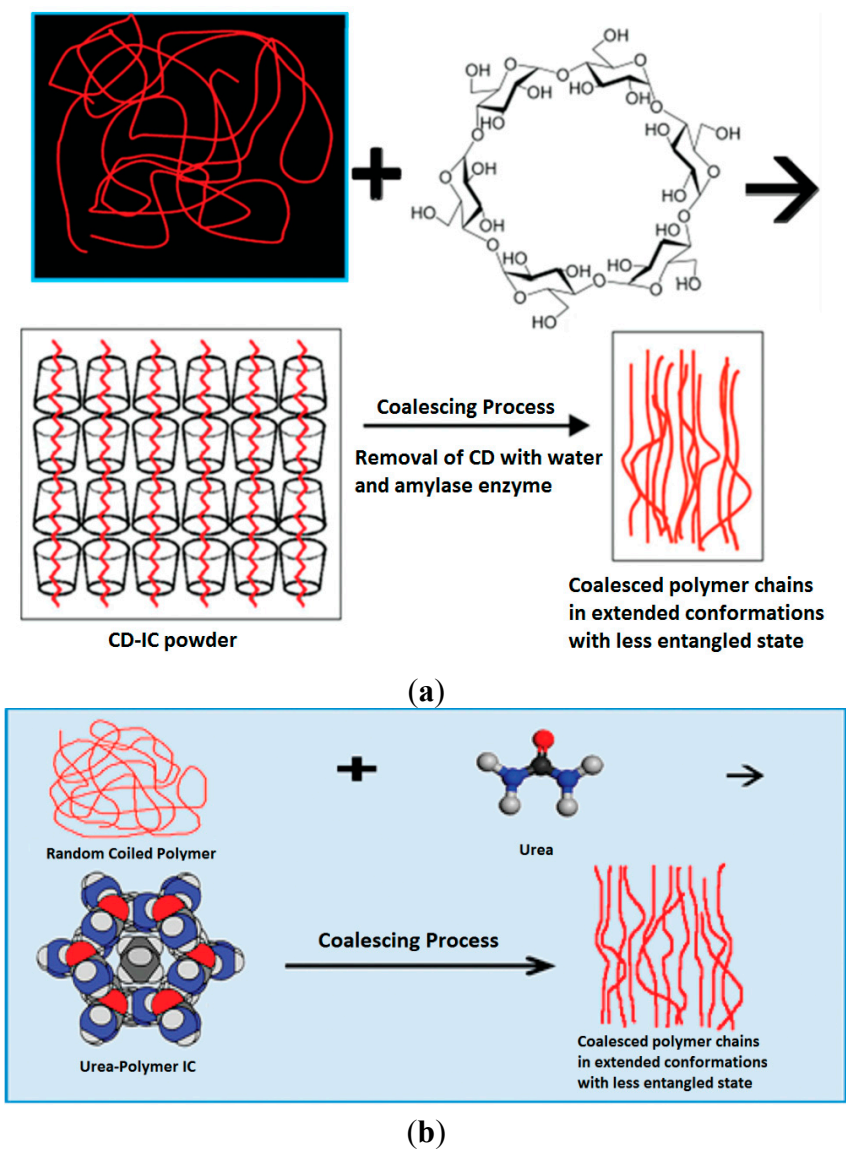


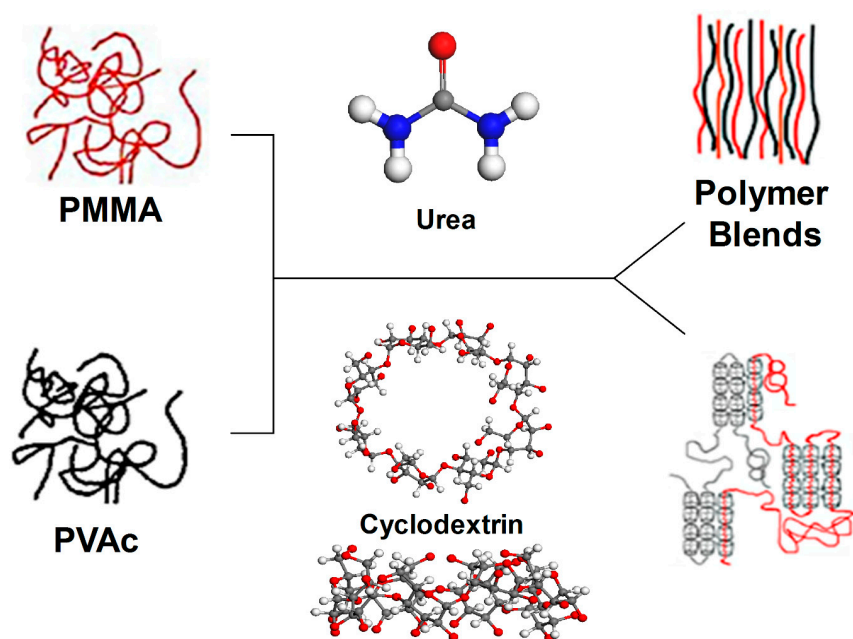
**Figure 6.** Formation and coalescence from CD (a) and U (b) polymer ICs [32].



### 3.2. Amorphous Polymers Coalesced from Their Stoichiometric and (n-s)-CD-ICs

Behaviors of amorphous polymers threaded through and coalesced from their (n-s)-CD-ICs and stoichiometric CD- and U-ICs (see Figure 7) have also been blended/mixed and examined [32–34]. In general, the glass transition temperatures,  $T_g$ s, of amorphous guest polymers coalesced from their stoichiometric CD- and U-ICs and (n-s)-CD-ICs and those un-included chain portions in the (n-s)-CD-ICs exhibit significantly elevated  $T_g$ s. This is demonstrated [34] for atactic PVAc and PMMA in Figure 8. In addition, as observed and noted above for semi-crystalline guest polymers coalesced from their CD- and U-ICs, the  $T_g$ s of amorphous guest polymers coalesced from their CD- and U-ICs also remain elevated above those of their as-received samples even upon being annealed considerably above  $T_g$  for long periods of time. The  $T_g$ s of coalesced (c)-poly(vinyl acetates) (PVAc)s annealed at 70 °C for 0, 8, 14, and 28 days were 41.5, 41.7, 41.5, and 41.2° C, respectively [34].

**Figure 7.** Comparison of blending poly(methyl methacrylate) (PMMA) and poly(vinyl acetate) (PVAc) via coalescence from stoichiometric U-IC and formation of (n-s)- $\gamma$ -CD-ICs [34].



Mention should be made that the  $T_g$ s observed for asr- and c-PMMA are 83 and 97 °C and 110 and 124 °C, respectively, for samples with molecular weights of 15 and 350 kDa that were coalesced from their  $\gamma$ -CD- and U-ICs. Since these molecular weights are considerably below and above the entanglement molecular weight of PMMA, respectively [35], it is not surprising that the  $T_g$ s observed for their asr-samples differ by 27 °C. It does seem somewhat surprising, however, that their coalesced samples also have  $T_g$ s that differ by 27 °C. If the agreement of the  $T_g$  differences between asr- and c-PMMA samples with very divergent molecular weights is not fortuitous, then it may possibly indicate that the molecular weight dependence of polymer glass-transition temperatures is not sensitive to whether or not they are entangled, but rather to the concentration of their chain-ends [36]. The basis for this suggestion arises because c-polymer samples are believed to be comprised of largely extended and un-entangled chains, while the chains in asr-samples are randomly-coiling and entangled (see Figure 6). This is supported by the higher densities measured for c-PVAcS presented in Table 1.

Judging from the virtually identical densities measured for PVAc-coalesced from their  $\gamma$ -CD- and U-ICs both below and above their  $T_g$ s, it appears that the resulting organization and behavior of c-PVAc do not depend on the host crystalline lattice from which they were coalesced.

**Figure 8.** Differential scanning calorimetry (DSC) heating scans of c-PVAc and coalesced (c)-PMMA (from their U-ICs) and as-received (asr)-PMMA and asr-PVAc [34].

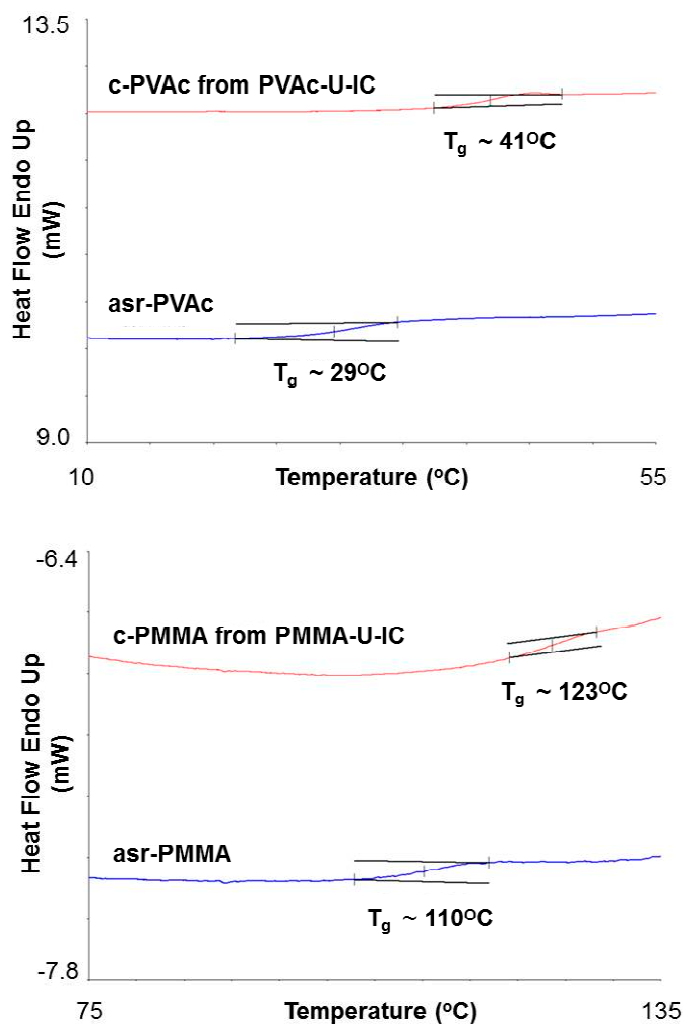


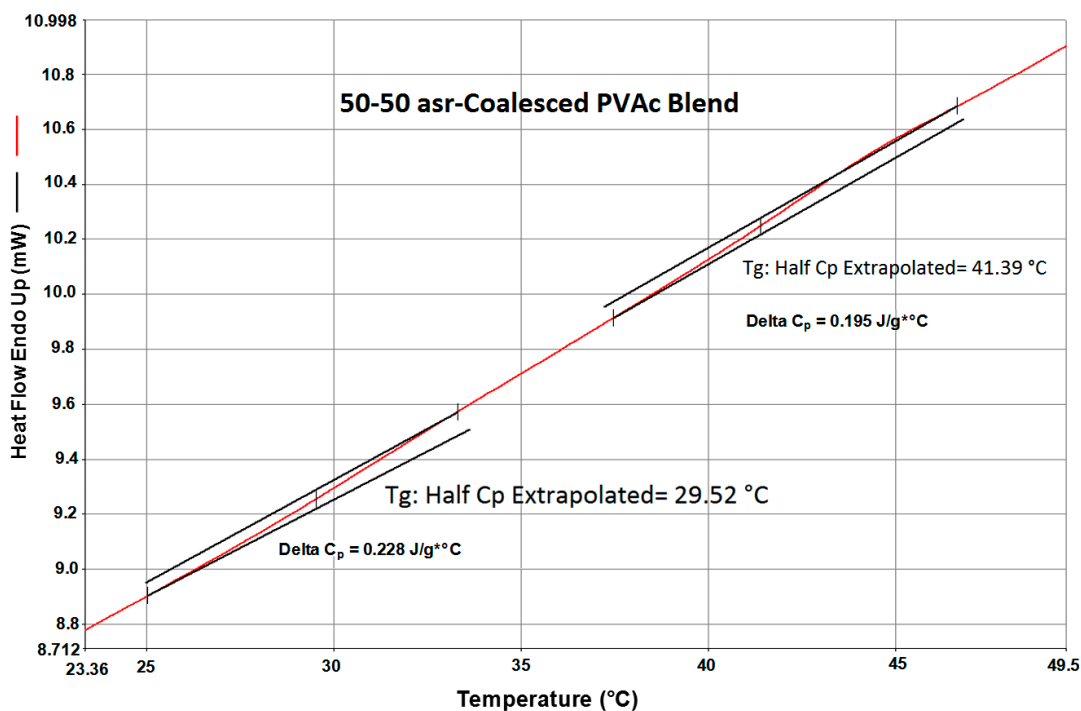
**Table 1.** Densities of asr- and c-PVAc measured below and above their  $T_g$ s [34].

Sample	Density at 25 °C ( $\text{g}/\text{cm}^3$ ) (below $T_g$ )	Density at 58 °C ( $\text{g}/\text{cm}^3$ ) (above $T_g$ )
asr-PVAc	1.093	1.040
c-PVAc ( $\gamma$ -CD)	1.156	1.077
c-PVAc (U)	1.154	1.076

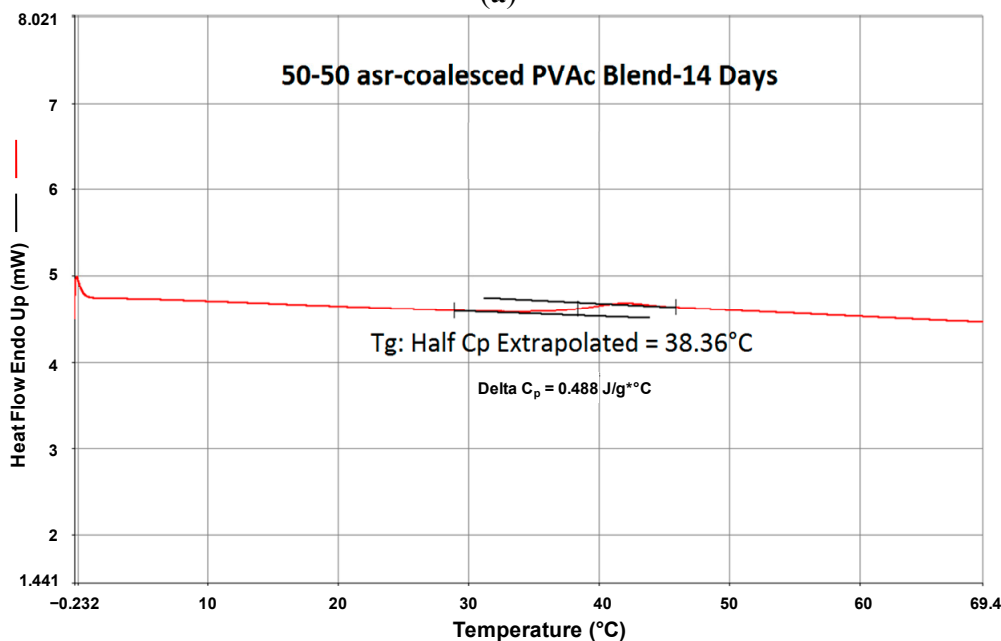
In a preliminary study, we made a 50:50 (wt:wt) mixture of asr- and c-PVAc and recorded its DSC heating scan, which is shown in Figure 9. There the  $T_g$ s of both asr- and c-PVAc can be seen. The sample pan was then removed from the DSC instrument and annealed in an oven at 70 °C for two weeks. The DSC heating scan for the annealed 50:50 asr/c-PVAc mixture was then measured and is also presented in Figure 9. A single  $T_g$  is observed and it is close to that of c-PVAc. It appears that long-term annealing above  $T_g$  has resulted in the reorganization of the asr-PVAc portion of the mixture

into that similar to the c-PVAc portion. The observation that the single  $T_g$  observed for the apparently well-mixed blend is close to that of c-PVAc, rather than asr-PVAc, is surprising. In other words, the blend is likely not characterized by completely entangled randomly-coiling PVAc chains, but rather by an organization of PVAc chains more similar to that of the initially coalesced neat c-PVAc ( $\gamma$ -CD). These preliminary DSC observations are supported by the densities that were measured for the asr- and c-PVAc and their 50:50 blend after annealing at 70 °C for two weeks, which were 1.044, 1.077, and 1.076 g/cm<sup>3</sup>, respectively.

**Figure 9.** DSC scans of an initial 50/50 physical mixture of asr-PVAc/c-PVAc (a) before and (b) after annealing for 14 days at 70 °C [34].



(a)



(b)

Currently we are annealing further the 50:50 mixture and have also begun annealing an 80:20 asr-PVAc:c-PVAc mixture at 70 °C to see if it also eventually is transformed/reorganized to that of a completely coalesced PVAc sample.

### 3.3. (N-S)-ICs with Amorphous Guest Polymers

(N-S)-CD-ICs were formed with amorphous PVAc and PMMA and examined by DSC [34]. Table 2 presents the  $T_g$ s measured for (n-s)-PVAc- $\gamma$ -CD-ICs with different stoichiometries, which lead to distinct lengths of uncovered un-included PVAc chain portions, as well as those of asr- and c-PVAc. There it is seen that the constrained un-included PVAc chain portions in (n-s)- $\gamma$ -CD-ICs have higher  $T_g$ s than neat asr- and c-PVAc samples. Furthermore, as the lengths of the un-included chain portions are shortened it appears that their  $T_g$ s increase as a consequence of the increasing constraint placed on them by their included chain portions. Similar observations were made on (n-s)-, asr-, and c-PMMA [34].

**Table 2.**  $T_g$ s of (n-s)-PVAc- $\gamma$ -CD-ICs [34].

Sample	PVAc (g)	$\gamma$ -CD (g)	$T_g$ (°C)
asr-PVAc	–	–	28
c-PVAc	–	–	41
2:1 (n-s)-IC	0.369	0.928	49
3:1 (n-s)-IC	0.369	0.615	49
6:1 (n-s)-IC	1.107	0.928	44

Very recently Mano *et al.* [37,38] reported (n-s)- $\alpha$ -CD-ICs made with amorphous atactic guest poly L,D-(lactic acid) (PLDLA). For a ~7:1 (n-s)-PLDLA- $\alpha$ -CD-IC they reported a  $T_g$  for the un-included portions of the guest PLDLA chains that was only ~5 °C above that of their neat PLDLA sample. On the other hand, we observed [34] and have mentioned above, that the  $T_g$ s of the un-included chain portions of atactic PVAc and PMMA in their (n-s)- $\gamma$ -CD-ICs to be at least as high as those of their coalesced bulk samples, which in turn are more than 10 °C above their asr-samples. Because Mano *et al.* [37,38] used 2-, 3-, and 4-fold excesses of PLDLA over the stoichiometric amount for full coverage by  $\alpha$ -CD, they likely ended up with both excess free PLDLA and stoichiometric PLDLA- $\alpha$ -CD-IC in their sample, which would explain the nearly identical  $T_g$ s they reported for their IC and neat PLDLA samples.

There are two ways of producing partially compatible PVAc/PMMA blends. The first involves formation of stoichiometric common  $\gamma$ -CD- or U-ICs [33,39] and the second the formation of common (n-s)- $\gamma$ -CD-ICs [34]. Coalescence from common stoichiometric ICs yields neat blends, while in common (n-s)- $\gamma$ -CD-ICs the blending occurs between the un-included portions of PVAc and PMMA chains. Previously PMMA/PVAc intimately mixed blends were obtained by formation and coalescence of their common  $\gamma$ -CD-ICs [37,38]. This was done using lower molecular weight PVAc (~13 kDa) and PMMA (~15 kDa). These coalesced blends showed some miscibility above the  $T_g$  of PVAc, where PVAc chains are able to diffuse in to PMMA domains.

In Figure 10 DSC data for PMMA/PVAc blends coalesced from their common U-ICs with varying initial PMMA:PVAc (70/30, 50/50, and 30/70) mol% ratios are presented, where all heating scans exhibit three  $T_g$ s. The lower and higher  $T_g$ s ( $T_{g1}$  and  $T_{g2}$ ) correspond to those of neat PVAc and

PMMA, respectively, coalesced from their U-ICs. This indicates that the polymer chains in the coalesced blends are largely aligned similar to the coalesced homopolymers processed with U. In between these two  $T_{g}$ s, there is an intermediate  $T_{g\text{-miscible}}$ , which corresponds to the miscible phase.

From the DSC scans it can be concluded that  $T_{g\text{-miscible}}$  moves toward the  $T_g$  of PVAc with increasing initial PVAc content. The compositions of the phases corresponding to  $T_{g\text{-miscible}}$  was estimated using the Fox Equation [40–42] (below) and are presented in Table 3 and Figure 11. This analysis confirms preferential inclusion of PMMA over PVAc [34,37,38] and indicates that in order to get an approximate equimolar mixture in a coalesced PMMA/PVAc blend an initial PVAc/PMMA composition of 70/30, or close to 2:1, in the feed is required:

$$(T_{g\text{-miscible}})^{-1} = W_{\text{PVAc}}/T_{g\text{PVAc}} + W_{\text{PMMA}}/T_{g\text{PMMA}}$$

**Figure 10.** DSC heating scans of PMMA/PVAc blends coalesced from their stoichiometric U-ICs [34].

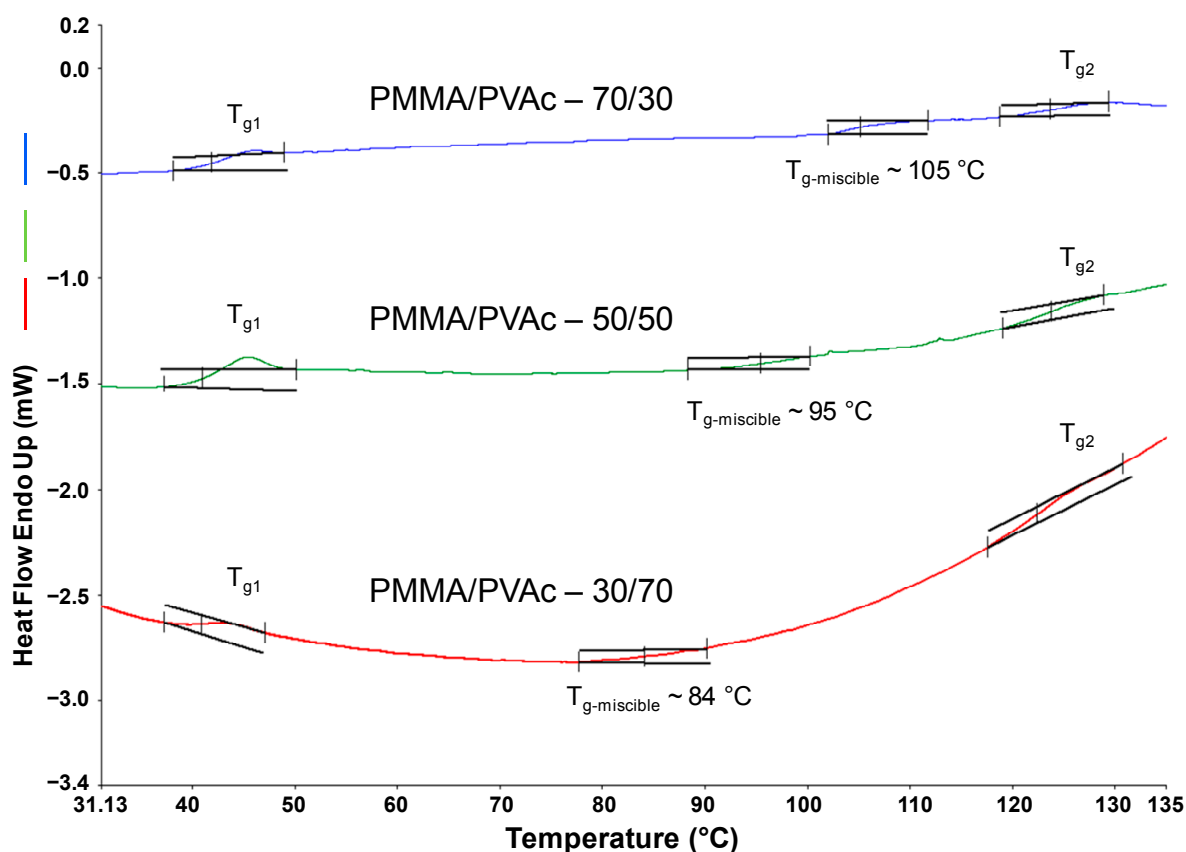
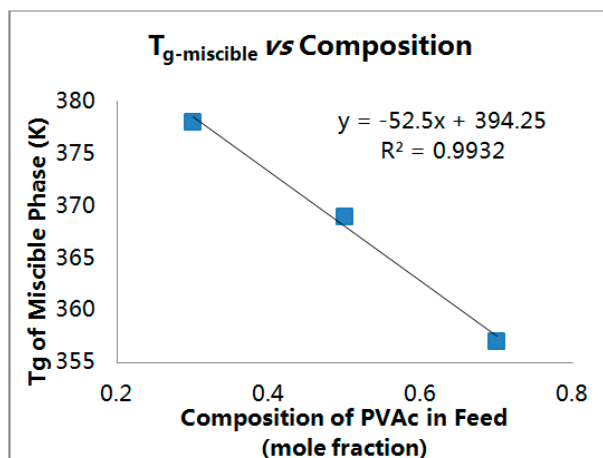


**Table 3.**  $T_{g\text{-miscible}}$ s of PMMA/PVAc blends coalesced from their stoichiometric U-ICs [34].

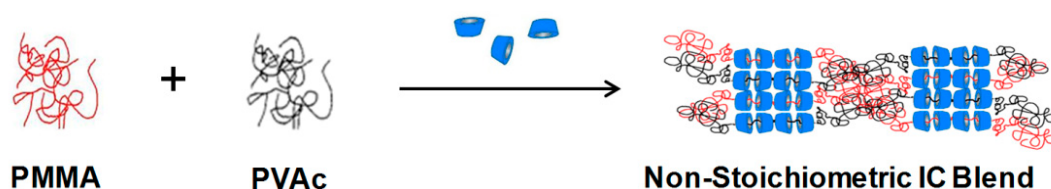
Feed		Blend	
PVAc/PMMA (mol%)	$T_{g\text{-miscible}}$ (K)	PVAc (mol%)	PMMA (mol%)
30/70	378	21	79
50/50	369	31	69
70/30	357	46	54

**Figure 11.**  $T_{g\text{-miscible}}$  observed (■) for PMMA/PVAc blends coalesced from their stoichiometric U-ICs [34], using the Fox Equation [40–42] to obtain the straight line.

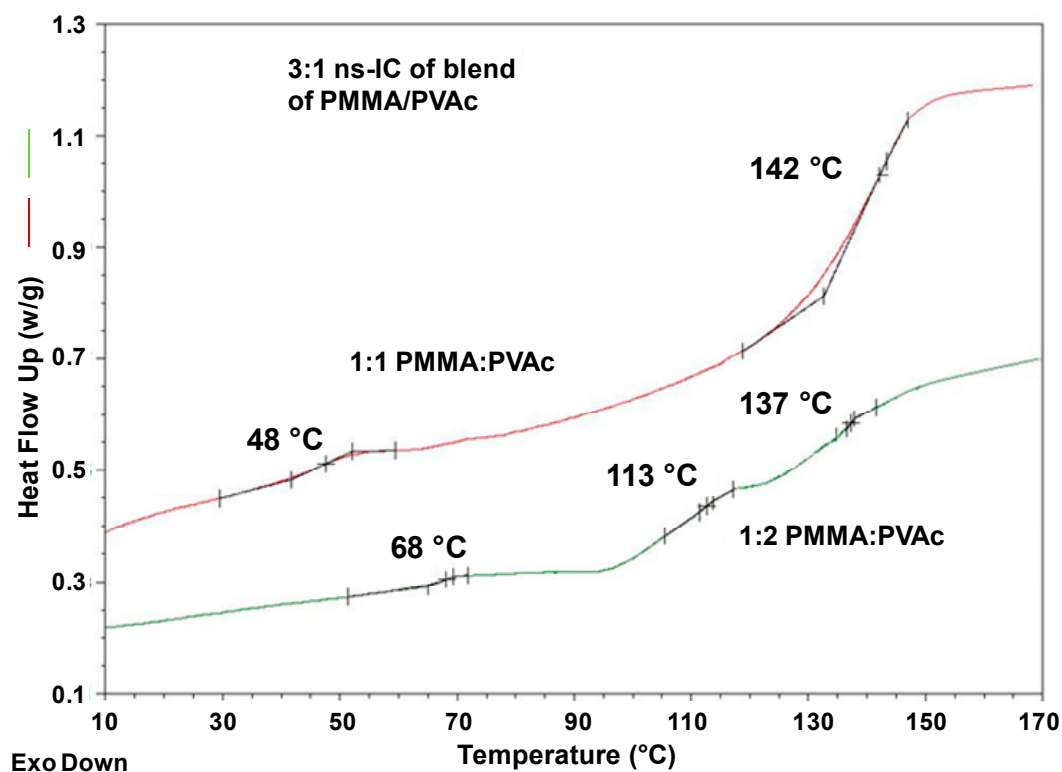


PMMA/PVAc can also be partially blended using  $\gamma$ -CD as a compatibilizer through formation of their common non-stoichiometric (n-s)-c-CD-ICs [32], as shown in Figure 12. We prepared (n-s)- $\gamma$ -CD-ICs with 2:1, 3:1, and 6:1 ratios of the polymer pair to  $\gamma$ -CD and 1:1 and 1:2 PMMA:PVA stoichiometries, which were confirmed with  $^1\text{H-NMR}$  to be in agreement with the starting proportions of PVAc, PMMA, and  $\gamma$ -CD.

**Figure 12.** Blending of un-included portions of PMMA and PVAc chains in their common (n-s)- $\gamma$ -CD-ICs [34].



DSC results for the common 3:1 (n-s)-PVAc/PMMA- $\gamma$ -CD-IC blends are shown in Figure 13 and summarized in the Table 4. For the 1:1 PMMA/PVAc initial mixture, we observe the glass transition temperatures for PVAc and PMMA at 48 and 143 °C, respectively, similar to the  $T_g$ s obtained for the neat 3:1 (n-s)-ICs of PVAc and PMMA. This indicates that the common 3:1 (n-s)-PMMA/PVAc(1:1)- $\gamma$ -CD-IC contains distinct  $\gamma$ -CD-IC crystals including exclusively each of the neat guest polymers. We can also see in Table 4, that unlike the  $T_g$ s of the neat (n-s)- $\gamma$ -CD-ICs, which simply shifted to higher temperatures, in the case of the common 3:1 (n-s)-PVAc/PMMA- $\gamma$ -CD-IC, with 2:1 PVAc:PMMA stoichiometry, they move closer to each other, indicating a certain degree of mixing between the “dangling” un-included PVAc and PMMA chain portions. Although the mixing is far from complete, as indicated by a  $T_g$  close to that of the neat 3:1 (n-s)-PMMA- $\gamma$ -CD-IC, the difference in the other two  $T_g$ s observed in relation to both the as-received and coalesced polymers is an indication of the presence of PMMA chains in PVAc-rich domains and *vice versa*.

**Figure 13.** Heating DSC scans of common 3:1 (n-s)-PVAc/PMMA- $\gamma$ -CD-ICs [34].**Table 4.**  $T_g$ s observed in common (n-s) PMMA/PVAc- $\gamma$ -CD-ICs.

(n-s)-IC Sample (Polymer: $\gamma$ -CD)	PMMA/PVAc Molar Ratio	$T_{g1}$ (°C)	$T_{g2}$ (°C)	$T_{g3}$ (°C)
3:1	1:1	48	–	142
3:1	1:2	68	113	137

Thus, we get hardening (higher  $T_g$ ) of PVAc caused by the presence and partial mixing of PMMA, and softening (lower  $T_g$ ) of the PMMA from the presence and partial mixing of PVAc, resulting in a decrease of its glass transition temperature, compared to both asr- and c-PMMA. More interesting is the observation of an intermediate  $T_g$  at 113 °C, which is consistent with a well-mixed phase containing similar amounts of un-included portions of PVAc and PMMA chains.

At this point it may be useful to compare the softening temperatures ( $T_g$ s) of the “dangling” un-included portions of amorphous guest polymer chains in (n-s)-CD-ICs with those in high density brushes tethered to solid surfaces. Before making the comparison we must emphasize that at least some of the un-included portions of guest polymer chains in (n-s)-CD-ICs are constrained at both ends as they emerge from one and enter another or a nearby CD-IC crystal channel (see Figures 2 and 12). This suggests that host CDs thread over both ends of the guest chains during IC formation. In polymer brushes, on the other hand, polymer chains are covalently bonded to solid surfaces at only one chain end. However, as mentioned previously, the surface densities of chains in polymer brushes and the un-included chains emanating from the CD-IC crystal surfaces in (n-s)-CD-ICs can be similar [7,18,20].

Above, we observed elevations as large as ~15–20 °C in the  $T_g$ s of un-included PVAc and PMMA chain portions in their (n-s)- $\gamma$ -CD-ICs above the  $T_g$ s of their neat bulk samples. Dense PMMA [20] and polystyrene (PS) [43] brushes covalently attached to silicon wafers both show elevated glass-transition temperatures ( $T_g$ s ~ 10–25 °C higher than the values observed for their neat bulk samples), but only



for thin brushes, with vertical heights in the ranges <50–100 nm. The elevations in glass-transition temperatures over those of their amorphous neat bulk samples observed for polymer chain portions un-included and constrained in (n-s)-CD-ICs and in thin dense brushes tethered to silicon wafers appear to be similar.

Based on their  $M_{WS}$  (167,000 and 350,000, respectively) and assuming full chain extension, the un-included chain portions in 2:1 (n-s)-PVAc- and PMMA-CD-ICs are on average ~250 and 450 nm. This is much longer than the <50–100 nm thickness of thin tethered PMMA and PS brushes that show elevated  $T_g$ s [20,43]. Tethered PMMA and PS brushes with thicknesses of 250–400 nm comparable to the lengths of un-included PVAc and PMMA chains in their (n-s)- $\gamma$ -CD-ICs do not show elevated  $T_g$ s. This suggests that the constraints placed on both ends of un-included PVAc and PMMA chains emerging from and entering into different CD-IC crystals are more severe than the packing constraints placed on high density brushes more than 50–100 nm above the surface of their attachment.

The importance of the constraints placed on both ends of at least some un-included chains portions in (n-s)-CD-ICs receives additional support from their necessary contribution to the “shape-memory” of these materials [4–7,9]. This strongly suggests that somewhere in the middle portions of the doubly tethered un-included chains there exit regions where they are not highly extended, but “randomly-coiled”, as in singly tethered high density polymer brushes far above their surface of attachment, and are able to be readily extended. Nevertheless, the likely presence of these less extended, less densely packed regions do not cause a reduction in their  $T_g$ s to those of their bulk samples, as is the case in high density, singly tethered, thick polymer brushes. With respect to the glass-transition temperatures of amorphous polymers in their (n-s)-CD-ICs, apparently the constraint of double-attachment/tethering of their un-included portions outweighs the effect of extensional flexibility in their “randomly-coiling” regions.

#### 4. Summary and Conclusions

We have described and compared the behaviors of the un-included guest polymer chains in (n-s)-polymer-CD-ICs to those exhibited by their bulk samples, by samples coalesced from their ICs, by their dense brushes, and in common (n-s)-CD-ICs containing two different guest polymers. Using higher  $T_c$ s or  $T_g$ s as criteria, the constraints placed on the un-included portions of polymer chains in their (n-s)-CD-ICs are at least equal and usually greater than those in their bulk, coalesced, and dense brush samples. This is apparently a consequence of at least some un-included chain portions in (n-s)-CD-ICs being tethered at both ends, rather than tethering at a single chain end in polymer brushes. On the other hand, in common (n-s)-CD-ICs containing two different amorphous guest polymers, which are at least partially mixed, the guest polymer with the lower  $T_g$  shows a  $T_g$  increased above that of its neat (n-s)-CD-IC, and *vice versa* for the common guest polymer with the higher bulk  $T_g$ .

#### Acknowledgments

I am grateful to the many students, in particular Abhay Jojode, and colleagues whose work constituted the bulk of this review and whose names can be found in several of the references listed below. Of course the invitation from the editor of this special issue, William J. Brittain, is also appreciated.

## Conflicts of Interest

The author declares no conflict of interest.

## References

1. Huang, L.; Tonelli, A.E. Polymer inclusion compounds. *J. Macromol. Sci. C Polym. Rev.* **1998**, *38*, 781–837.
2. He, Y.; Inoue, Y.  $\alpha$ -Cyclodextrin-enhanced crystallization of poly(3-hydroxybutyrate). *Biomacromolecules* **2003**, *4*, 1865–1867.
3. Vogel, R.; Tandler, B.; Haussler, L.; Jehnichen, D.; Brunig, H. Melt spinning of poly(3-hydroxybutyrate) fibers for tissue engineering using  $\alpha$ -cyclodextrin/polymer inclusion complexes as the nucleation agent. *Macromol. Biosci.* **2006**, *6*, 730–736.
4. He, Y.; Inoue, Y. Effect of  $\alpha$ -cyclodextrin on the crystallization of poly(3-hydroxybutyrate). *J. Polym. Sci. B Polym. Phys.* **2004**, *42*, 3461–3469.
5. Dong, T.; He, Y.; Zhu, B.; Shin, K.; Inoue, Y. Nucleation mechanism of  $\alpha$ -cyclodextrin-enhanced crystallization of some semicrystalline aliphatic polymers. *Macromolecules* **2005**, *38*, 7736–7744.
6. Dong, T.; Shin, K.; Zhu, B.; Inoue, Y. Nucleation and crystallization behavior of poly(butylene succinate) induced by its  $\alpha$ -cyclodextrin inclusion complex: Effect of stoichiometry. *Macromolecules* **2006**, *39*, 2427–2428.
7. Shin, K.; Dong, T.; He, Y.; Inoue, Y. Morphological change of poly( $\epsilon$ -caprolactone) with a wide range of molecular weight via formation of inclusion complex with  $\alpha$ -cyclodextrin. *J. Polym. Sci. B Polym. Phys.* **2005**, *43*, 1433–1440.
8. Mohan, A.; Joyner, X.; Kotek, R.; Tonelli, A.E. Constrained/directed crystallization of nylon-6. I. nonstoichiometric inclusion compounds formed with cyclodextrins. *Macromolecules* **2009**, *42*, 8983–8991.
9. Mohan, A.; Gurarlan, A.; Joyner, X.; Child, R.; Tonelli, A.E. Melt-crystallized nylon-6 nucleated by the constrained chains of its non-stoichiometric cyclodextrin inclusion compounds and the nylon-6 coalesced from them. *Polymer* **2011**, *52*, 1055–1062.
10. Gurarlan, A.; Tonelli, A.E. Single-component polymer composites. *Macromolecules* **2011**, *44*, 3856–3861.
11. Gurarlan, A.; Shen, J.; Tonelli, A.E. Single-component poly( $\epsilon$ -caprolactone) composites. *Polymer* **2013**, *54*, 5747–5753.
12. Tonelli, A.E. Restructuring polymers via nanoconfinement and subsequent release. *Beilstein J. Org. Chem.* **2012**, *8*, 1318–1332.
13. Tonelli, A.E. Molecular processing of polymers with cyclodextrins. *Adv. Polym. Sci.* **2009**, *222*, 55–77.
14. Lide, D.R. *Handbook of Chemistry & Physics*, 85th ed.; CRC Press: Boca Raton, FL, USA, 2004.
15. Mohan, A. Modification of Nylon-6 Structure via Nucleation. Ph.D. Thesis, North Carolina State University, Raleigh, NC, USA, 12 August 2009.
16. Shin, D.I.; Huang, L.; Tonelli, A.E. NMR observation of the conformations and motions of polymers confined to the narrow channels of their inclusion compounds. *Macromol. Symp.* **2011**, *138*, 21–40.

17. Dong, T.; Kai, W.; Pan, P.; Cao, A.; Inoue, Y. Effects of host–guest stoichiometry of  $\alpha$ -cyclodextrin–aliphatic polyester inclusion complexes and molecular weight of guest polymer on the crystallization behavior of aliphatic polyesters. *Macromolecules* **2007**, *40*, 7244–7251.
18. Tsujii, Y.; Ohno, K.; Yamamoto, S.; Goto, A.; Fukada, T. Structure and properties of high-density polymer brushes prepared by surface-initiated living radical polymerization. *Adv. Polym. Sci.* **2006**, *197*, 1–45.
19. Gechele, G.B.; Crescentini, L. Melting temperatures and polymer–solvent interaction for polycaprolactam. *J. Appl. Polym. Sci.* **1963**, *7*, 1349–1357.
20. He, G.-L.; Merlitz, H.; Sommer, J.-U.; Wu, C.-X. Polymer brushes near the crystallization density. *Eur. Phys. J. E* **2007**, *24*, 325–330.
21. Tonelli, A.E. Calculation of the intramolecular contribution to the entropy of fusion in crystalline polymers. *J. Chem. Phys.* **1970**, *52*, 4749–4751.
22. Tonelli, A.E. On the existence of local segmental order in undiluted bulk polymers. *J. Chem. Phys.* **1970**, *53*, 4339–4345.
23. Tonelli, A.E. Intramolecular and intermolecular contributions to the fusion of linear aliphatic polyesters and polyamides and their effects on the observed differences in polyester and polyamide melting temperatures. *J. Chem. Phys.* **1971**, *54*, 4637–4641.
24. Tonelli, A.E. Intramolecular contributions to the entropy and energy of fusion of polyethyleneoxalate and polyethylenesuccinate. *J. Chem. Phys.* **1972**, *56*, 5533–5535.
25. Tonelli, A.E. Fusion as an opportunity for calorimetrically probing polymer conformations and interactions in the bulk state. In *Analytical Calorimetry*; Porter, R.S., Johnson, J.F., Eds.; Plenum: New York, NY, USA, 1974; Volume 3, p. 89.
26. Tonelli, A.E. Polyethylene and polytetrafluoroethylene crystals: Chain folding, entropy of fusion and lamellar thickness. *Polymer* **1976**, *17*, 695–698.
27. Tonelli, A.E. Melting of aliphatic nylons. *J. Polym. Sci. B Polym. Phys.* **1977**, *15*, 2051–2053.
28. Lee, H.; Jakubowski, W.; Matyjaszewski, K.; Yu, S.; Shieko, S.S. Cylindrical core–shell brushes prepared by a combination of ROP and ATRP. *Macromolecules* **2006**, *39*, 4983–4989.
29. Trujillo, M.; Arnal, M.L.; Muller, A.J.; Laredo, E.; Bredeau, S.; Bonduel, D.; Dubois, P. Thermal and morphological characterization of nanocomposites prepared by *in situ* polymerization of high-density polyethylene on carbon nanotubes. *Macromolecules* **2007**, *40*, 6268–6276.
30. Yang, P.; Han, Y. Microphase-separated brushes on square platelets in PS-*b*-PEO thin films. *Macromol. Rapid Commun.* **2009**, *30*, 1509–1514.
31. Yu-Su, S.Y.; Sheiko, S.S.; Lee, H.; Jakubowski, W.; Nese, A.; Matyjaszewski, K.; Anokhin, D.; Ivanov, D.A. Crystallization of molecular brushes with block copolymer side chains. *Macromolecules* **2009**, *42*, 9008–9017.
32. Gurarslan, A.; Shen, J.; Tonelli, A.E. Behavior of poly( $\epsilon$ -caprolactone)s (PCLs) coalesced from their stoichiometric urea inclusion compounds and their use as nucleants for crystallizing PCL melts: Dependence on pcl molecular weights. *Macromolecules* **2012**, *45*, 2835–2840.
33. Rusa, C.C.; Wei, M.; Suuai, X.; Bullions, T.A.; Wang, X.; Rusa, M.; Uyar, T.; Tonelli, A.E. Molecular mixing of incompatible polymers through formation of and coalescence from their common crystalline cyclodextrin inclusion compounds. *J. Polym. Sci.* **2004**, *42*, 4207–4224.

34. Joojode, A.S.; Antony, G.J.; Tonelli, A.E. Glass-transition temperatures of nanostructured amorphous bulk polymers and their blends. *J. Polym. Sci. B Polym. Phys.* **2013**, *51*, 1041–1050.
35. Wool, R.P. Polymer entanglements. *Macromolecules* **1993**, *26*, 1564–1569.
36. Fox, T.G.; Flory, P.J. The glass temperature and related properties of polystyrene—Influence of molecular weight. *J. Polym. Sci.* **1954**, *14*, 315–319.
37. Oliveira, T.; Botelho, G.; Alves, N.M.; Mano, J.F. Inclusion complexes of-cyclodextrin with poly(D,L-lactic acid):structural characterization and glasstrabsition dynamics. *Colloid Polym. Sci.* **2014**, *292*, 863–871.
38. Viciosa, M.T.; Alves, N.M.; Oliviera, T.; Dionisio, M.; Mano, J.F. Confinement effects on the dynamic behavior of poly(D,L-lactic acid) upon incorporation in  $\alpha$ -cyclodextrin. *J. Phys. Chem. B* **2014**, *118*, 6972–6981
39. Uyar, T.; Rusa, C.C.; Wang, X.; Rusa, M.; Hacaloglu, J.; Tonelli, A.E. Intimate blending of binary polymer systems from their common cyclodextrin inclusion compounds. *J. Polym. Sci.* **2005**, *43*, 2578–2593.
40. Fox, T.G., Jr.; Flory, P.J. 2nd-order transition temperature and related properties of polystyrene. 1. influence of molecular weight. *J. Appl. Phys.* **1950**, *21*, doi:10.1063/1.1699711.
41. Fox, T.G. Influence of diluent and of copolymer composition on the glass temperature of a polymer system. *Bull. Am. Phys. Soc.* **1956**, *1*, 123.
42. DiMarzio, E.A.; Gibbs, J.H. Glass temperature of copolymers. *J. Polym. Sci.* **1959**, *40*, 121–131.
43. Tate, R.S.; Fryer, D.S.; Pasqualini, S.; Montague, M.F.; dePaola, J.J.; Nealey, P.F. Extraordinary elevation of the glass transition temperature of thin polymer films grafted to silicon oxide substrates. *J. Chem. Phys.* **2001**, *115*, doi:10.1063/1.1415497.

© 2014 by the authors; licensee MDPI, Basel, Switzerland. This article is an open access article distributed under the terms and conditions of the Creative Commons Attribution license (<http://creativecommons.org/licenses/by/3.0/>).